Numerical analysis of moment-deflection response in hybrid steel-GFRP reinforced concrete beams

Ravshanbek Mavlonov [a)], Kamoliddin Muminov, Abdurasul Martazaev, Sohiba Numanova, Odiljon Fozilov

Namangan State Technical University, Namangan, Uzbekistan

[a)] *Corresponding author: ravshanbek.mavlonov@gmail.com*

Abstract. In this article, the moment-deflection behavior of six types of hybrid steel-GFRP reinforced concrete beams and three types of conventional steel reinforced concrete beams was studied using ANSYS numerical modeling. A total of nine beam types were tested and classified into three groups, each containing one control specimen steel reinforced concrete beams to compare with the hybrid steel-GFRP beams. The obtained results demonstrate that the load-carrying capacity and deflection characteristics of the hybrid reinforced concrete beams are nearly equivalent to those of the traditional steel-reinforced beams.

INTRODUCTION

Nowadays, in the global construction sector, increasing the load-carrying capacity of structures, reducing their self-weight, and developing technically, economically, and environmentally efficient solutions have become increasingly urgent tasks [1]. Even though steel rebar, widely used in reinforced concrete structures, possesses high strength, its susceptibility to corrosion, greater self weight, and high cost are becoming the main issue to certain limitations in some applications [2-3].

Corrosion of steel reinforcement in reinforced concrete structures reduces the integrity and service life of the structure. When steel corrodes, it causes to cracking in concrete structures and reduces the bond strength between the rebar and concrete, ultimately decreasing the load-carrying capacity and potentially leading to failure [4-5]. The corrosion process in reinforced concrete happens in the presence of water and oxygen, as well as chloride ions originating from seawater or de-icing salts. Once steel begins to corrode, the resulting chemical products penetrate throughout the concrete matrix, causing cracking within the concrete [6-8].

Concrete is a material with particular physical, mechanical properties and susceptible to crack. Electrolytes can go through capillaries and reach the reinforcement due to the interconnection of internal voids and microcracks. Under favorable environmental conditions, dissolved chloride ions (Cl) and carbon dioxide (CO_2) increase the likelihood of corrosion [9-11]. Carbonation of concrete and the infiltration of chloride ions alter the pore structure within concrete. Such conditions influence the galvanic mechanism responsible for protecting steel reinforcement, thereby accelerating corrosion. Additionally, carbonation caused by the penetration of CO_2 which creates an acidic environment, and in the presence of chloride ions, corrosion of steel may occur through deteriorated zones [12-14].

As the construction industry develops, extensive research is being conducted on methods of protecting steel reinforcement from corrosion to extend the service life of reinforced concrete elements. One hands-on solution to this issue is replacing steel bar with a corrosion resistant reinforcement. In this context, FRP reinforcement has become an important and reliable alternative [15]. It is electrically non-conductive, diamagnetic and non-corrosive, which makes it suitable for structures in harsh environments. It is a desirable choice because of its advantageous strength to weight ratio, which lowers the self-weight of structures. Additionally, FRP helps lessen the risk of thermal cracking in concrete structures since it has a lower coefficient of thermal expansion than steel [16-17].

Although the design of concrete structures reinforced with FRP bars, is addressed in the codes of several countries, the brittle nature of FRP reinforcement prevents it from being recommended as a complete substitute for steel reinforcement [18]. Instead, the concept of hybrid steel-FRP reinforcement in concrete elements has been proposed.

Steel reinforcements provide ductility to hybrid reinforced concrete beams, and FRP bars increase the total structural load-bearing capacity due to their better tensile strength. This approach helps mitigate the risk of brittle failure in only FRP reinforced concrete beams [19-21].

METHODOLGY

Current engineering practice, numerical modeling software based on the finite element method are widely used worldwide to study the stress-strain state, load-carrying capacity, crack resistance and its mitigation, as well as deformation behavior of structural elements, including beams. This technique makes it possible to effectively integrate experimental and theoretical analyses. ANSYS Workbench software is unique features for its high efficiency, accuracy, and powerful functional capabilities in modeling, especially reinforced concrete structures.

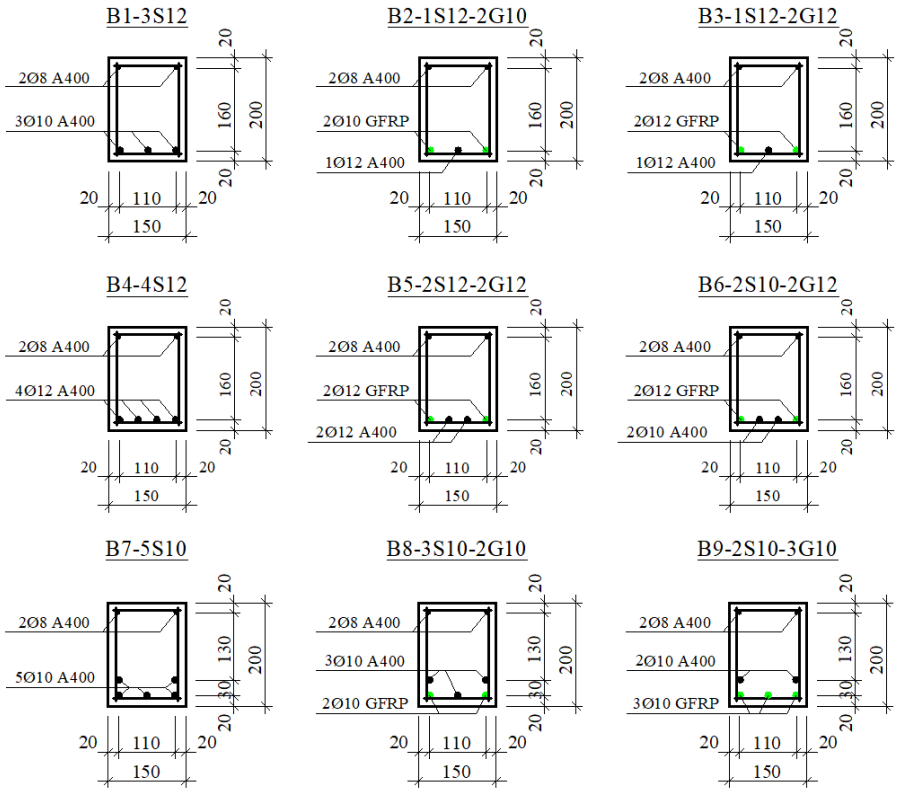

FIGURE 1. Cross-sections of the beams and arrangement of the reinforcement cages

A total of nine beams were divided into three groups based on the number of reinforcements placed in the tension zone [6, 9].

Group 1 beams (B1-3S12, B2-1S12-2G10, and B3-1S12-2G12) were reinforced with three bars in the tensile region. B1-3S12 beam served as the control beam for this group and was reinforced with steel bars. Specimens B2-1S12-2G10 and B3-1S12-2G12 were hybrid steel-GFRP reinforced concrete beams, in which two GFRP bars with diameters of 10 mm and 12 mm, respectively, were installed at the corners (Figure 1).

Group 2 beams (B4-4S12, B5-2S12-2G12, and B6-2S10-2G12) were reinforced with four bars placed in a single row within the tensile zone. B4-4S12 was the conventional steel reinforced control beam, while specimens B5-2S12-2G12 and B6-2S10-2G12 were hybrid reinforced concrete beams. In these two beams, two GFRP bars with a diameter of 12 mm were positioned at the corners, while the central bars were steel bars with diameters of 12 mm and 10 mm, respectively (Figure 1).

Group 3 beams (B7-5S10, B8-3S10-2G10, and B9-2S10-3G10) were reinforced with five bars arranged in two rows in the tension zone. When reinforcement bars were arranged longitudinally in two layers, the vertical spacing between the layers was set to 30 mm. In beams B8-3S10-2G10 and B9-2S10-3G10, steel and GFRP bars were used in a combined manner. All beams in Group 3 had the same reinforcement ratio. In specimen B8-3S10-2G10, 10-mm-

diameter GFRP bars were placed at the corners, whereas in specimen B9-2S10-3G10, all three bars located closest to the tensile surface were made of composite reinforcement (Figure 1).

The length of the beams was $l=150$ *cm* and an effective length was of $l_0=140$ *cm*. The beams had a rectangular cross-section with dimensions $b\times h=15\times 20$ *cm*. The applied concentrated load was positioned at a distance of $l_0/3$ from the supports. The distance from the beam end to the support was 5 cm. All beams were tested under normal (flexural) section behavior. The beams were reinforced with reinforcement cages. Since the beams were designed to be tested in flexure, no transverse reinforcement was placed in the central region of the span. In the near the supports, the spacing of the stirrups was set to 5 cm. The total length of the reinforcement cage was 145 cm, and its height was 18 cm. All beams were reinforced with two Ø8 mm A400 steel bars in the compression zone. Ø6 mm A240 steel bars were used as stirrups [6, 9].

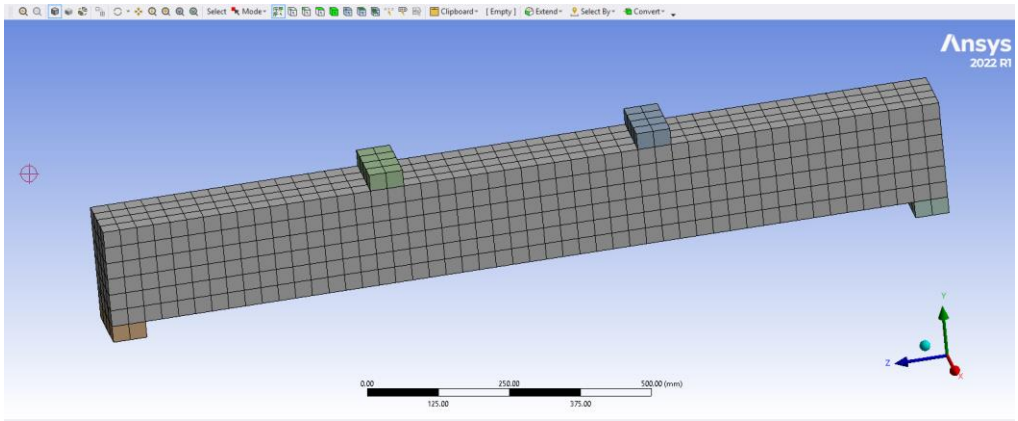

FIGURE 2. Modeling of the beam in ANSYS and its discretization into finite elements

Within the scope of this study, the nonlinear behavior of both concrete and reinforcement was taken into account during the numerical modeling of the beams. For concrete, the plasticity and crack formation characteristics were considered using the Drucker-Prager model, while for steel and composite reinforcement, post-yield inelastic deformations were modeled. This approach made it possible to more accurately reflect the actual working conditions of the structure and to obtain reliable results.

In the ANSYS Workbench, the beam geometry was discretized into finite elements. To ensure computational accuracy, linear (hexahedral) elements with a size of 25 mm were selected for meshing (Figure 2).

RESEARCH RESULTS

Particular attention was given to ensuring the accuracy and reliability of the results obtained through digital modeling of the beams using ANSYS. For this purpose, the model was developed based on the results of laboratory experimental tests. Specifically, the measured laboratory data related to beam deformation, stress-strain behavior, and deflection were compared with the results obtained from ANSYS. Comparative analyses demonstrated that the experimental and numerical results were consistent and supported each other. The reliability of the numerical results was increased through the proper selection of model parameters and design schemes, as well as the accurate incorporation of the physical and mechanical properties of concrete and reinforcement. Consequently, an accurate model was built, capable of serving as a basis for further analyses and structural design solutions. This significantly contributes to increasing the efficiency of prediction and design processes in practical engineering.

In the analysis of flexural elements according to the second group of limit states, deflection is the most critical deformation parameter. Figures 3, 4, and 5 present the deflection values corresponding to the applied load on the beams.

Series 1 specimens.

As shown in the load-deflection diagram (Figure 3), steel reinforcements in the tensile zone of traditional concrete beams (B1-3S12) exhibits a distinctly defined yield point associated with the onset of yielding in the steel reinforcement. When the applied load reached $0.88P_u$, the steel bars transitioned into the plastic range, and at this stage a mid-span deflection was 3.80 mm. As the loading continued beyond the yield point, the beam underwent larger deflections, indicating the development of plastic hinges and a significant reduction in stiffness due to post yield

strength of steel reinforcement. Ultimately, at the maximum load-carrying capacity, the deflection was 15.15 mm under a load of P_u=106.6 kN, indicating ductile behavior of conventional steel reinforced concrete beams.

For the hybrid steel-GFRP reinforced specimens (B2-1S12-2G10 and B3-1S12-2G12), the initial response differed substantially due to the combined steel and GFRP bars in the tensile zone of concrete. Both hybrid beams behaved elastically at (0.21…0.23)P_u, similar to the traditional reinforced concrete beam, maintaining stable stiffness during the early loading phases because of the presence of steel rebar. As the applied load increased, the deflection rose simultaneously, reflecting the influence of the lower elastic modulus of GFRP reinforcement. With equivalent deflections of 3.34 mm for B2-1S12-2G10 and 3.27 mm for B3-1S12-2G12, yielding of the steel reinforcement was noted when the load was (0.48–0.53)P_u. These values show that the hybrid beams experienced slightly smaller deflections at the onset of steel yielding compared to the steel reinforced concrete beam, owing to the partial stiffness contribution of the GFRP bars.

In comparison to the B1-3S12 beam, the hybrid beams generated much greater deflections at the ultimate load-carrying capacity. A deflection of 21.36 mm at P_u=100.2 kN in B2-1S12-2G10, while B3-1S12-2G12 had 17.79 mm at P_u=106.5 kN. These higher deflections are mainly due to the linear-elastic behavior of the GFRP bars, which do not yield but continue to deform until rupture. As a result, the hybrid beams are able to undergo greater displacement before failure.

Furthermore, because the reinforcement ratio in specimen B2-1S12-2G10 was slightly lower than in the other specimens, its deflection at ultimate load exceeded that of B3-1S12-2G12 by 3.57 mm. A reduced reinforcement ratio generally contributes to increase the flexural resistance of the section, allowing more effective utilization of the tensile capacity of the FRP reinforcement. This behavior is consistent with the observed increase in deflection in specimen B2-1S12-2G10.

It is also noteworthy that the ultimate load-carrying capacities of the hybrid-reinforced beams were essentially equivalent to that of the conventional steel-reinforced beam with the same overall reinforcement quantity. Despite this similarity in load carrying capacity, the difference in ultimate deflection between hybrid steel-GFRP reinforced concrete beams and traditional reinforced concrete beam was 2.64 mm, indicating an enhanced deformation capacity in the hybrid beams. This behavior is clearly reflected in the load–deflection curves shown in Figure 3.

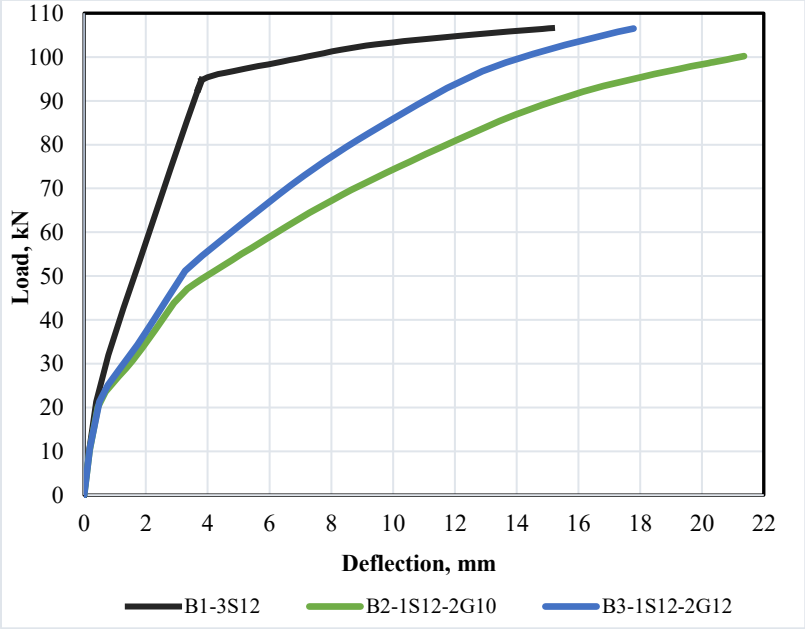

FIGURE 3. Load–deflection diagram for Series 1 beams

Series 2 specimens.

The load–deflection response indicated that when the applied load reached 0.95P_u in conventional steel reinforced concrete beam, the steel reinforcement still remained within the elastic range, and the corresponding mid-span deflection was 4.07 mm. The beam showed a deflection of 9.01 mm when the applied load reached its highest value of P_u=129.10 kN, indicating a comparatively little deflection at beam failure.

In contrast, the hybrid steel-GFRP reinforced concrete beams (B5-2S12-2G12 and B6-2S10-2G12) showed linear-elastic behavior up to (0.20…0.22)P_u due to steel reinforcement receiving initial loads in the beam, consistent with the elastic nature of GFRP reinforcement. Yielding of the steel bars occurred at load of 0.71P_u and 0.56P_u, with corresponding deflections of 3.63 mm and 3.27 mm, respectively. These values show earlier steel yielding compare to steel reinforced concrete beam, primarily due to the reduced stiffness contribution associated with GFRP bars.

At the ultimate limit state, the hybrid beams exhibited larger deflections compared to the steel reinforced concrete beam. Specimen B5-2S12-2G12 reached the maximum deflection of 13.52 mm when applied load was P_u=118.57 kN, while specimen B6-2S10-2G12 had the largest deflection of 15.90 mm at P_u=110.70 kN. The increased deflections of the hybrid steel-GFRP reinforced concrete beams can be attributed to the comparatively lower modulus of elasticity of the GFRP reinforcement and differences in reinforcement ratio.

The steel-reinforced beam reached an ultimate load that was 10.53 kN higher than that of the hybrid specimens, while its ultimate deflection was 4.51 mm smaller, according to a study of beams with equal total reinforcement ratios. According to these findings, the steel-reinforced beam in Series 2 demonstrated better structural performance than the hybrid steel-GFRP beams, as evidenced by its greater load-carrying capacity and less deformation (Figure 4). This behavior is consistent with the mechanical advantages of steel reinforcement, including higher stiffness and the ability to yield before failure.

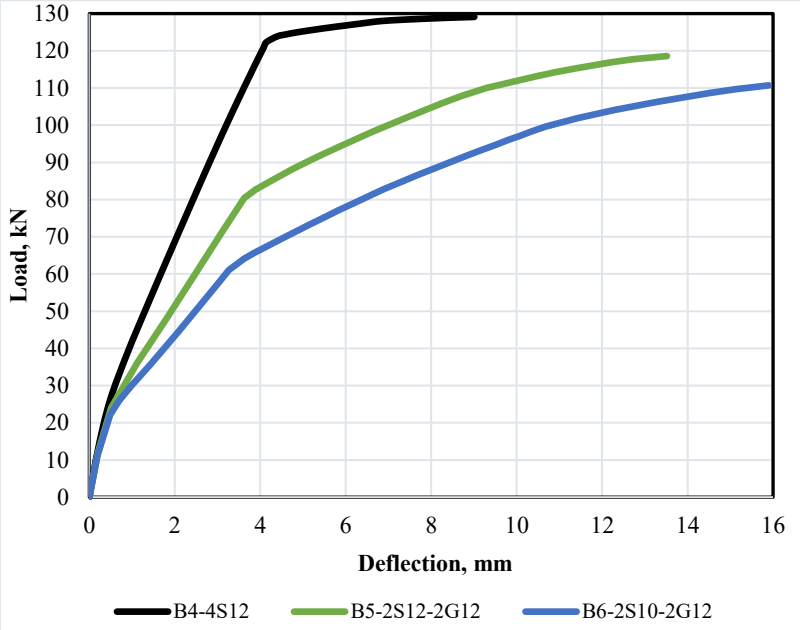

FIGURE 4. Load–deflection diagram for Series 2 beams

Series 3 specimens.

For the control specimen B7-5S10, which was reinforced with five steel bars in the tension zone, the load–deflection diagram indicated that the beam maintained elastic behavior up to 0.93P_u. Once normal stress in the steel reinforcement reached its yield strength, a noticeable increase in deflection observed in the beam. The mid-span deflection changed from 4.74 mm to 13.98 mm, while the load-bearing capacity rose from P=100.02 kN to P=107.05 kN. This behavior reflects the typical post-yield ductility of traditional steel reinforced concrete beams, where deflection continues to rise even with relatively small values of applied load.

For the hybrid steel-GFRP reinforced beams (B8-3S10-2G10 and B9-2S10-3G10), an approximately linear elastic response was observed up to the load range of (0.20…0.22)P_u, similar to the earlier series. This elastic response is consistent with the existence of GFRP reinforcements in the beam. The steel rebar yielding occurred at 0.69P_u and 0.57P_u, with corresponding deflections of 4.43 mm and 4.26 mm, respectively. Following steel yielding, both hybrid beams exhibited a substantially accelerated increase in deflection. At the ultimate failure stage, the beams reached loads of 105.52 kN and 102.10 kN, with deflections of 18.31 mm and 15.89 mm, respectively.

In Series 3, the difference in load-bearing capacity between fully steel reinforced concrete beam and hybrid steel-GFRP reinforced concrete beams was relatively small, ranging from 1.4% to 4.6%. However, the difference in ultimate deflection was slightly larger, ranging from 12% to 24%. These results show that even though hybrid reinforced beams

are capable of achieving load capacities comparable to steel reinforced beams, they exhibit significantly greater deflection. Moreover, increasing GFRP reinforcement ratio within the hybrid beams led to a further increase in deflection. This trend is associated with the lower elastic modulus of GFRP rebar compared to steel bar, which results in reduced response and as a result, greater deflections under similar loading (Figure 5).

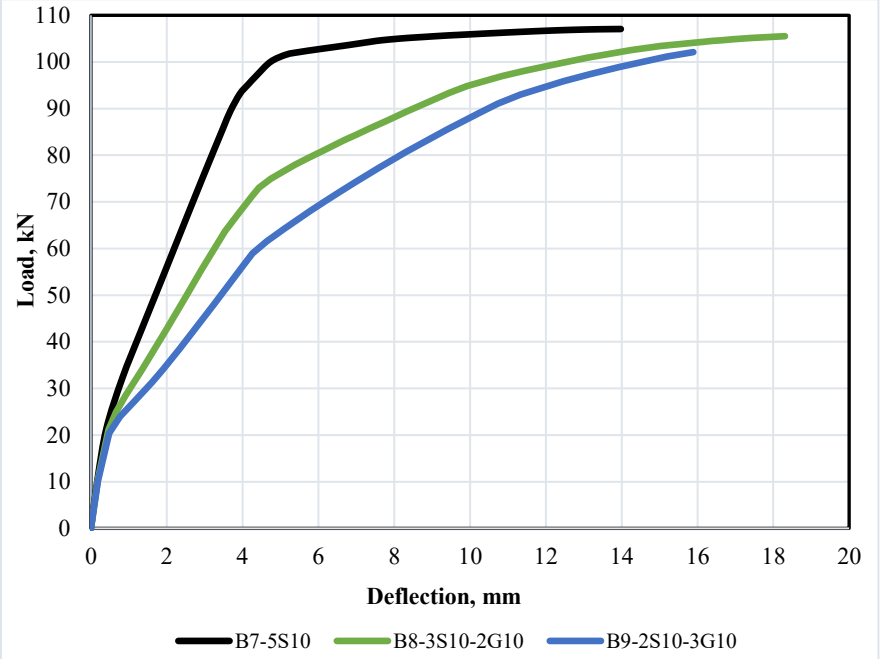

FIGURE 5. Load–deflection diagram for Series 3 beams

A comprehensive analysis of the numerical outcomes obtained from Series 1, Series 2, and Series 3 provides a clear understanding of the flexural behavior of traditional steel reinforced and hybrid steel-GFRP reinforced concrete beams. The comparative evaluation presents the influence of both steel and GFRP reinforcements placement, reinforcement ratio, and the contribution of GFRP bars on the overall stiffness, ductility, crack resistance and load-bearing capacity of the beams.

In all series, conventional steel reinforced concrete beams showed elastic behavior according to Hooke's law up to relatively high load, between (0.88…0.95) P_u, before the steel reinforcement reached its yield point. In contrast, the hybrid steel-GFRP reinforced concrete beams demonstrated elastic behavior only up to approximately (0.20…0.23)P_u due to the presence of GFRP bars which have different mechanical properties. This earlier transition from elastic to inelastic stage in the hybrid beams is primarily associated with nearly four times less the lower modulus of elasticity of GFRP reinforcement, which results in reduced initial stiffness and earlier redistribution of tensile stresses toward the steel bars. Consequently, yielding of steel in hybrid steel-GFRP reinforced concrete beams was observed earlier, typically loads ranging from $0.48P_u$ to $0.71P_u$ depending on the reinforcement ratio.

Significant differences were also observed in the deflection behavior of the both beams. The traditional steel reinforced concrete beams presented small deflection at the first group of limit state, values generally range 9 mm and 15 mm. Hybrid beams demonstrated slightly higher deflections at failure, typically within the range of 15 mm to 22 mm. This increase is associated with the elastic behavior and low elastic modulus of GFRP rebar compared to steel bar. In each series, beams including a higher GFRP reinforcement ratio than that of steel experienced larger mid-span deflections. Therefore, increasing the amount of GFRP reinforcement directly influences flexural strength of the concrete beams.

In spite of these differences in stiffness and deflections, load-carrying capacities of hybrid steel-GFRP reinforced concrete beams were found to be comparable to those of conventional steel reinforced concrete beams. In Series 1, the difference in ultimate load between hybrid and steel reinforced beams was not large, typically between 0.1 kN and 6.4 kN. In Series 2, the steel-reinforced beam exhibited higher load capacity by approximately 10.5 kN, which can be attributed to its higher reinforcement ratio. In Series 3, the difference in load-carrying capacity ranged from 1.4% to

4.6%. These results show that partial replacement of steel by GFRP reinforcement, the hybrid reinforced concrete beams retained approximately 90–98% of the load-bearing strength of conventional steel reinforced concrete beams.

The influence of reinforcement ratio and configuration was clearly seen in all three series. Lower reinforcement ratios or with a higher amount of GFRP rebar in the hybrid reinforced concrete beams showed early steel bar yielding, greater mid-span deflections, and slightly reduced load-bearing capacities. These techniques show that the flexural response of hybrid beams is controlled by the interaction between the steel yielding as well as the linear-elastic behavior and modulus of elasticity of the GFRP bars. However, the hybrid steel-GFRP reinforced concrete beams exhibited adequate strength and ductility, indicating that placing steel and GFRP reinforcements in the tension zone of the beams can be achieved without significant reductions in ultimate strength.

CONCLUSIONS

Overall, the comparative analysis in all three series leads to some important conclusions. First, load-carrying capacities of hybrid steel-GFRP beams are nearly equal to conventional steel reinforced beams, confirming this approach is applicable in construction. Second, the use of GFRP reinforcement with steel reinforcement in the tension zone significantly increases deformability of the beams, which may be advantageous in terms of energy absorption and ductility. However, it must be carefully considered in serviceability limit states including deflection. Third, the overall performance of hybrid reinforced concrete beams depends on the ratio between steel and GFRP reinforcement to ensure a suitable balance between load-bearing capacity, stiffness, and crack control.

The obtained results confirm that hybrid steel-GFRP reinforced concrete beams can be an alternative solution to traditional steel reinforced beams, offering a combination of high strength, sufficient ductility, and improved durability, especially in environments where corrosion resistance is critically important.

REFERENCES

1. Nguyen P.D., Dang V.H., Vu N.A. Performance of concrete beams reinforced with various ratios of hybrid GFRP/steel bars // Civil Engineering Journal. Vol. No 9:1652–1669. https://doi.org/10.28991/cej-2020-03091572
2. Bingyan Wei, Xiongjun He, Ming Zhou, Huayi Wang, Jia He. Experimental study on flexural behaviors of FRP and steel bars hybrid reinforced concrete beams. Case Studies in Construction Materials 20 (2024) e02759, https://doi.org/10.1016/j.cscm.2023.e02759
3. Ahmed El Refai, Farid Abed, Abdullah Al-Rahmani. Structural performance and serviceability of concrete beams reinforced with hybrid (GFRP and steel) bars. Construction and Building Materials 96 (2015) 518–529, http://dx.doi.org/10.1016/j.conbuildmat.2015.08.063
4. Z. Sun, L. Fu, D. Feng, A. R. Vatuloka, Y. Wei and G. Wu, Flexural behavior of concrete beams reinforced with bundled hybrid steel/FRP bars, Eng. Struct. 197, 109443 (2019); https://doi.org/10.1016/j.engstruct.2019.109443.
5. Hawileh, R., Finite element modeling of reinforced concrete beams with a hybrid combination of steel and aramid reinforcement, Materials and Design (2014), doi: http://dx.doi.org/10.1016/j.matdes.2014.10.004
6. Ravshanbek Mavlonov, and Sobirjon Razzakov. Numerical modeling of combined reinforcement concrete beam. E3S Web of Conferences 401, 03007 (2023) CONMECHYDRO – 2023. https://doi.org/10.1051/e3sconf/202340103007
7. Seongeun Kim & Seunghun Kim (2019): Flexural Behavior of Concrete Beams with Steel Bar and FRP Reinforcement, Journal of Asian Architecture and Building Engineering, https://doi.org/10.1080/13467581.2019.1596814
8. Kara I.F., Ashour, A.F., Köroğlu, M.A., Flexural behavior of hybrid FRP/steel reinforced concrete beams // Composite Structures – 2015, http://dx.doi.org/10.1016/j.compstruct.2015.03.073
9. Ravshanbek Mavlonov, Sobirjon Razzakov, and Sohiba Numanova. Stress-strain state of combined steel-FRP reinforced concrete beams. E3S Web of Conferences 452, 06022 (2023) IPFA 2023, https://doi.org/10.1051/e3sconf/202345206022
10. Ruan, X., Lu, C., Xu, K., Xuan, G., Ni, M., Flexural behavior and serviceability of concrete beams hybrid-reinforced with GFRP bars and steel bars, Composite Structures (2019), doi: https://doi.org/10.1016/j.compstruct.2019.111772
11. M. A. Aiello and L. Ombres, Structural performances of concrete beams with hybrid (FRP-steel) reinforcements, J. Compos. Constr. 6, 133 (2002); https://doi.org/10.1061/(ASCE)1090-0268(2002)6:2(133)

12. A. Martazaev and S. Khakimov, “Dispersed reinforcement with basalt fibers and strength of fiber-reinforced concrete beams,” AIP Conf. Proc. 3256, 030011 (2025). https://doi.org/10.1063/5.0266797
13. W. Ge, J. Zhang, D. Cao and Y. Tu, Flexural behaviors of hybrid concrete beams reinforced with BFRP bars and steel bars, Constr. Build. Mater. 87, 28 (2015); https://doi.org/10.1016/j.conbuildmat.2015.03.113
14. Gu Xingyu, Dai Yiqing, Jiang Jiwang. Flexural behavior investigation of steel-GFRP hybrid-reinforced concrete beams based on experimental and numerical methods. Engineering Structures 206 (2020) 110117, https://doi.org/10.1016/j.engstruct.2019.110117
15. M. A. Safan, Flexural behavior and design of steel-GFRP reinforced concrete beams, ACI Mater. J. 110, 677 (2013); https://doi.org/10.14359/51686335
16. Devaraj, R.; Olofinjana, A.; Gerber, C. Making a Case for Hybrid GFRP-Steel Reinforcement System in Concrete Beams: An Overview. Appl. Sci. 2023, 13, 1463. https://doi.org/10.3390/app13031463
17. Yang Yang, Ze-Yang Sun, Gang Wu, Da-Fu Cao and Zhi-Qin Zhang. Flexural capacity and design of hybrid FRP-steel-reinforced concrete beams, Advances in Structural Engineering 1–15, 2019. https://doi.org/10.1177/1369433219894236
18. A. Martazaev, M. Orzimatova, and M. Xamdamova, “Determination of optimum quantity of silica fume for high-performance concrete,” AIP Conf. Proc. 3256, 030012 (2025). https://doi.org/10.1063/5.0266799
19. Hiep Dang Vu, Duy Nguyen Phan. Experimental and Theoretical Analysis of Cracking Moment of Concrete Beams Reinforced with Hybrid Fiber Reinforced Polymer and Steel Rebars. Advances in Technology Innovation, vol. 6, no. 4, 2021, pp. 222-234. https://doi.org/10.46604/aiti.2021.7330
20. S. Razzakov and A. Martazaev, Mechanical properties of concrete reinforced with basalt fibers, E3S Web Conf. 401, 05003 (2023); https://doi.org/10.1051/e3sconf/202340105003
21. Lau D., Pam H.J. Experimental study of hybrid FRP reinforced concrete beams // Engineering Structures, Vol. 32. – 2010. – p. 3857-3865. https://doi.org/10.1016/j.engstruct.2010.08.028